ELSEVIER

Physica C 247 (1995) 252–262

PHYSICA C

Carbon in $YBa_2Cu_3O_{7-x}$: origin and effects

F.J. Gotor [a], N. Pellerin [a], P. Odier [a,*], E. Cazy [b], J.P. Bonnet [b], A.R. Fert [c], J. Ayache [*,d,1]

[a] *Centre de Recherches sur la Physique des Hautes Températures, CNRS. 1D, Avenue de la Recherche Scientifique, 45071 Orléans Cedex 2, France*

[b] *LMCTS-ENSCI. 87065 Limoges Cedex, France*

[c] *Laboratoire de Physique des Solides (CNRS URA 74), INSA. Complexe Scientifique de Rangueil, 31077 Toulouse, France*

[d] *Laboratoire de Physique des Matériaux, CNRS. 1, Pl Aristide Briand, 92195 Meudon Cedex, France*

Received 17 January 1995; revised manuscript received 28 February 1995

Abstract

Residual carbon content in powders, sintered ceramics and textured samples was determined. Its source was shown to be essentialy the starting material precursors. Carbon content may be reduced to below 600 ppm if no liquid phase is formed during precursor processing. The case of samples processed by solidification from a liquid is important. In samples textured on MgO substrate, carbon is supplied by this substrate. In this case, liquid phase plays an active role on the carbon retention in the $YBa_2Cu_3O_{7-x}$ structure during crystallisation. Magnetic susceptibility behaviour of textured samples was analysed and discussed in relation to the presence of carbon. A qualitative correlation between the superconducting transition width and the carbon content was established. A sharp superconducting transition at 91.5 K was achieved when carbon content was less than 600 ppm.

1. Introduction

Obtaining high-quality $YBa_2Cu_3O_{7-x}$ superconducting ceramics requires a scrupulous control of the powder purity and processing conditions. It is well known that some powder synthesis methods, especially those based on carbon-containing precursors, produce $YBa_2Cu_3O_{7-x}$ powders with a broader transition temperature (several K) and generally an onset temperature (T_{conset}) below 92 K [1]. A similar degradation of superconducting properties reported in sintered $YBa_2Cu_3O_{7-x}$ ceramics has been attributed to deficient oxygenation [2]. Nevertheless, Shaw et al. [3] have proved that the difficulty in oxygenation is not the sole cause of this degradation. In addition, they suggested that the lowered and broadened transition observed in some powders and high-density ceramics may have a common origin, i.e. the retention of carbon in the $YBa_2Cu_3O_{7-x}$ structure. For their part, Masuda et al. [4] have demonstrated in $YBa_2Cu_3O_{7-x}$ powders synthesised by the sol–gel method a relationship between the presence of residual carbon and the lowering of T_{conset}. They showed that the higher T_{conset} was achieved when carbon content was reduced to 0.04 wt.% (400 ppm). A similar behaviour has been recently evidenced in the $Y_2Ba_4Cu_7O_{14+x}$ (247) phase

* Corresponding author.

[1] Present address: CSNM, Bat 108. Univ. Paris 11, 91405 Orsay Campus, France.

SSDI 0921-4534(95)00196-4

[5]. T_{conset} of this phase varies from 50 to 93 K as the content of carbon changes from 1200 to 100 ppm.

On the other hand, the segregation of carbon-rich second phases at grain boundaries in sintered ceramics as reported by several authors [6,7] is responsible for the degradation of intergrain properties, i.e. the critical current density. In any case, the temperature transition is depressed, as demonstrated by Rüffer et al. [8] in C–$YBa_2Cu_3O_{7-x}$ composite samples prepared by mixing $YBa_2Cu_3O_{7-x}$ and graphite powders. However, it has been suggested that a carbonate layer standing at the grain boundaries could act as a diffusion barrier in the reoxygenation process [7].

The carbon source is not limited to the starting materials, but also to the processing atmosphere because of the strong affinity of $YBa_2Cu_3O_{7-x}$ toward the CO_2 molecule [9–11]. Lindemer et al. [12] have shown that $YBa_2Cu_3O_{7-x}$ compound appears to take CO_2 into solution at 1173 K. Increasing CO_2 concentration in O_2 raises the incorporated carbon up to a limit content of 660 ppm, reached when 14000 ppm of CO_2 in pure O_2 flows above the sample. Higher CO_2 partial pressures produce the $YBa_2Cu_3O_{7-x}$ degradation. Karen et al. [13] have identified three oxycarbonates from the study of the pseudoternary system $Y(O/CO_3)$–$Ba(O/CO_3)$–$Cu(O/CO_3)$ at temperatures between 1053 and 1273 K in atmospheres containing oxygen and 5, 40 and 350 ppm CO_2. Recently, many other oxycarbonate phases have been reported in the Y–Ba–Cu–O system. Thus, Rodriguez et al. [14] have stabilised a phase with nominal composition $YBa_4Cu_2CO_3O_{5.5-x}$ by the presence of carbonate and they have established that this material is an oxycarbonate. Gotor et al. [15] have characterised a tetragonal phase, already reported in the preparation of $YBa_2Cu_3O_{7-x}$ from carbon-containing precursors [13,16], described as an Y–Ba–Cu oxycarbonate. Tetragonal phases with a similar X-ray powder diffraction pattern have been indicated as a consequence of CO_2 degradation of $YBa_2Cu_3O_{7-x}$ (at low partial pressures in pure oxygen) [12] and even in non-carbon-containing synthesis in flowing oxygen [17]. Finally, Boullay et al. [18] have synthesised two new phases, members of the series $Y_nBa_{2n}Cu_{3n-1}CO_3O_{7n-3}$, with $n = 2$, 3, which have a similar structure to that found in oxycarbonates of related systems such as (Y,Ca)–(Ba,Sr)–Cu–O [19,20] or Sr–Cu–O [21]. These papers illustrate well that carbon might be engaged into superconducting cuprate structure. The carbonate group strongly modifies the hole doping and generally results in degraded superconducting properties.

Preliminary studies concerning $YBa_2Cu_3O_{7-x}$ textured ceramics prepared by us using a modified MTG technique on MgO monocrystals never show the optimal T_{conset} otherwise observed when processing was made on an Y_2O_3 sintered substrate [22]. Note that the reoxygenation cycles were identical, suggesting that their magnetic behaviour may be not entirely due to a deficient oxygenation as often stated, but something else should be the cause of this difference.

In this work, the residual carbon content in powders, sintered ceramics and textured samples has been shown and quantitatively determined. Magnetic susceptibility behaviour of textured samples was also analysed and discussed in relation to the presence and origin of residual carbon. A qualitative correlation between carbon content and anomalies in magnetic susceptibility was found.

2. Experimental procedure

The different powders used in this study were prepared as follows: (i) pure $YBa_2Cu_3O_{7-x}$ powder obtained by firing a commercial precursor (Hoechst High Chem) in oxygen atmosphere at increasing temperatures (915–935°C) for 8 h in an alumina crucible with intermediate grinding in an agate mortar, (ii) commercial powder (Rhône-Poulenc, SUPERAMIC 123) partially degraded during its storage (two years); (iii) finally, three powders G1–G3 synthesised by the gel route [15,23]. This route consists in the gelation by an organic polymer of an aqueous nitrated solution containing all the required elements in the appropriate ratios; it is followed by the calcination of the as-obtained gel at 500°C in O_2 to produce a xerogel precursor. This xerogel was fired at 850°C in oxygen (G1), 800°C in argon (G2) and 925°C in oxygen (G3) and then (in all cases) slowly cooled in flowing oxygen. Every time, powder phase purity was characterised by X-ray diffraction (XRD) and differential scanning calorimetry (DSC).

Powder from Rhône-Poulenc was pressed into

pellets with a diameter of 10 mm. Pellets RP1 and RP2 were sintered respectively at 915 and 950°C in flowing oxygen (raising speed 10°C/min, dwelling time 12 h, cooling speed 10°C/min). For texturation, pure $YBa_2Cu_3O_{7-x}$ powder (from Hoechst) was isostatically pressed in to a disk shape ($\phi = 10$ mm, $h = 7$ mm) at 250 MPa and sintered at 935°C in oxygen (raising speed 2°C/min, dwelling time 8 h, cooling speed 2°C/min). These samples are called H1. The ceramic was then positioned on a single crystalline MgO or sintered Y_2O_3 substrate. The sample and its substrate were placed in a horizontal furnace where the longitudinal and radial thermal gradients are negligible. The heat treatment was made according to the profile of Fig. 1(a). A reoxygenation annealing under pure oxygen flow was made afterwards, following cycle a) of Fig. 1(b). All samples made in this study can be classified according to the substrate: T1, textured on fresh polished monocrystalline MgO; T2, textured on already used and not polished monocrystalline MgO; T3, textured on fresh polished and oxygen annealed (at 1200°C for 10 h) monocrystalline MgO; and T4, textured on polished polycrystalline Y_2O_3. It must be noticed

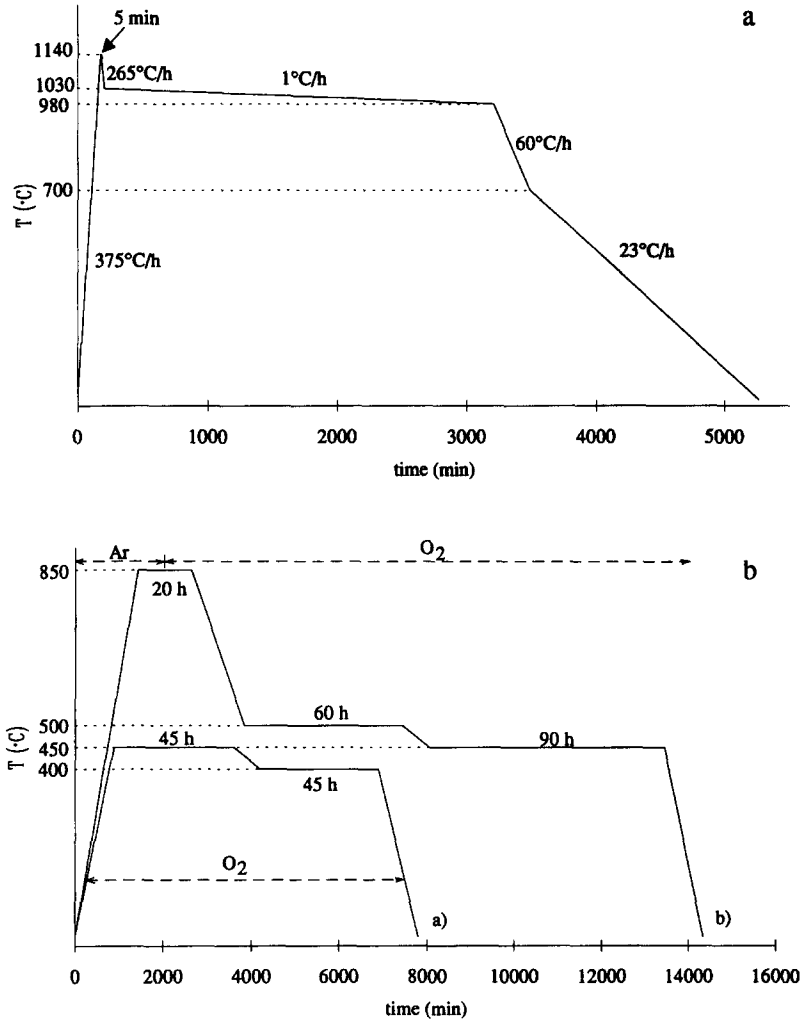

Fig. 1. (a) Temperature profile for the $YBa_2Cu_3O_{7-x}$ texturation, (b) classical reoxygenation procedure a) and modified reoxygenation procedure b) for $YBa_2Cu_3O_{7-x}$ textured samples.

that for an easier reading sample names reflect the sample origin: G, gel powder; RP, sintered ceramic from Rhône-Poulenc powder; H, sintered ceramic from Hoechst powder; and T, textured sample.

Carbon content analysis is based on the measurement of the amount of carbon dioxide evolved during the dissolution of $YBa_2Cu_3O_{7-x}$-based material in pure sulphuric acid. $YBa_2Cu_3O_{7-x}$ material was ground in an agate mortar just before its introduction into the glass vessel. After crossing the vessel, a constant buffer of nitrogen (PRODAIR, l'Oxygène Liquide, St Denis, France) was checked by a carbon dioxide infrared detector (Guardian II, ateliers NOEL, Provins, France) sensitive from 0 to 820 ppm of C. When zero signal was obtained, H_2SO_4 (Rhône-Poulenc, purity 95% minimum) was slowly poured till the total dissolution of the powder, observed for about 15 cm^3 of H_2SO_4 for 0.5 g of $YBa_2Cu_3O_{7-x}$. The amount of carbon contained in the starting material was then determined by integration of the CO_2 signal. The constant gas flow and the mass of $YBa_2Cu_3O_{7-x}$ material were adjusted to optimise the precision of the measurement. The detection limit was < 400 ppm and the measurement reproducibility was $\pm$ 100 ppm.

DC susceptibility measurements were carried out in a magnetic field of 1 mT using a SQUID magnetometer (Quantum Design).

Microstructures have been examined by analytical transmission electron microscopy (TEM) using a Jeol 2000FX equipped with EDX Link analyser.

3. Results

Residual carbon contents for $YBa_2Cu_3O_{7-x}$ powders obtained by the gel route and for the sintered ceramics (from Rhône-Poulenc and Hoechst) are shown in Table 1. Carbon in the gel powders is provided by he gel synthesis route [15]. Carbon content of these powders varies between 4000 and 700 ppm depending on calcination temperature and processing atmosphere. We had shown that G1 powder issued from this route and calcinated at 850°C in flowing oxygen is mainly constituted by a phase which remains tetragonal even after annealing ($\leq$ 850°C) in oxygen. However, their crystallographic parameters are comparable to those of the orthorhombic 123 phase. Recently, this phase has been characterised as an oxycarbonate [15]. From the nominal composition determined by refinement of the X-ray powder diffraction pattern — $YBa_2Cu_{2.95}(CO_3)_{0.35}O_{6.6}$ — this phase should contain 6200 ppm of carbon, which agrees with our determination, i.e. 4000 ppm, see Table 1. Other evidences of carbon in this powder was found by ELLS [24]. The existence of a carbonate-like environment has been shown by IR-spectroscopy [15]. This explains the fact that the G2 powder, annealed at 800°C in flowing Ar, presents lower carbon content that the G1 one in spite of a lower firing temperature. Obviously, the high-temperature treatment under neutral atmosphere helps carbonate-like dissociation as is well known for $BaCO_3$. Alternatively, vacuum treatment could be a good opportunity. An orthorhombic powder is obtained after treatment at higher temperatures in flowing oxygen (G3) or at 800°C under Ar followed by slow cooling in O_2 (G2).

Table 1
Carbon content in powders and sintered ceramics

Sample name	Sample origin	Thermal treatment	Carbon content (ppm)
G1	Gel powder	850°C in O_2	4000
G2	Gel powder	800°C in Ar	1300
G3	Gel powder	925°C in O_2	700
RP1	Rhône-Poulenc sintered ceramic	915°C in O_2	400
RP2	Rhône-Poulenc sintered ceramic	950°C in O_2	1600
H1	Hoechst sintered ceramic	935°C in O_2	600

Rhône-Poulenc degraded powder employed in RP ceramics contained 4090 ppm of carbon. Nevertheless, RP1 ceramic sintered at 915°C in O_2 only has 400 ppm of carbon. On the other hand, RP2 ceramic treated at 950°C presents a higher carbon content. This fact will be discussed later. Finally, H1 ceramic sintered at 935°C in O_2 also exhibits a rather low carbon content of 600 ppm. Generally, if powder precursor processing is realised carefully, i. e. precise control of firing temperature and atmosphere, carbon contents may be reduced to below 600 ppm. We can say that this carbon amount is the residual pollution for a $YBa_2Cu_3O_{7-x}$ powder designated as *pure*.

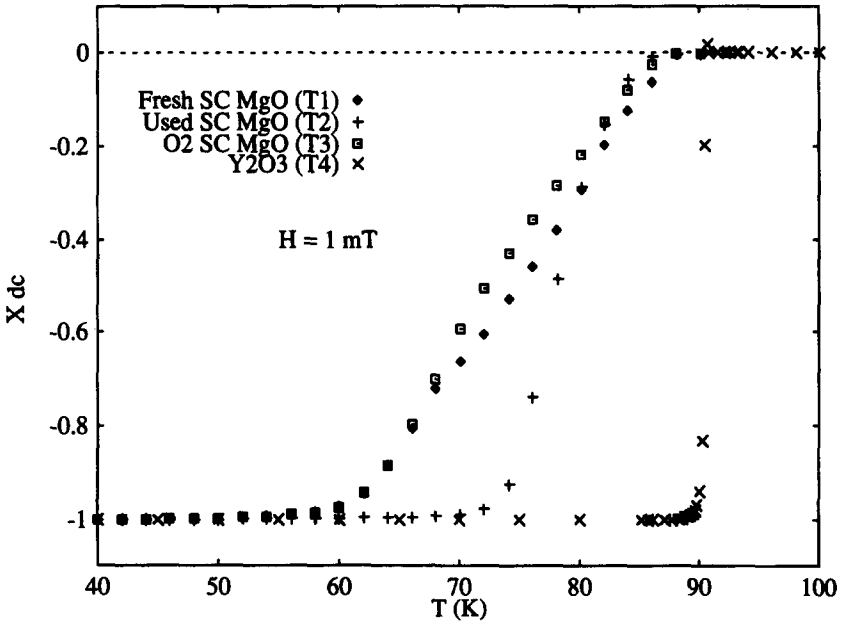

Fig. 2. ZFC magnetic susceptibility for $YBa_2Cu_3O_{7-x}$ textured samples after reoxygenation. T1, textured on fresh polished monocrystalline MgO; T2, textured on already used and not polished monocrystalline MgO; T3, textured on fresh polished and oxygen-annealed monocrystalline MgO and T4, textured on polished polycrystalline Y_2O_3.

As has been mentioned above, samples textured on MgO substrate are characterised by a broad transition even after long time reoxygenation. Comparison with samples textured on Y_2O_3 is interesting. As-grown samples have both a very broad transition and a low $T_{c\,onset}$: 70 K for samples textured on Y_2O_3

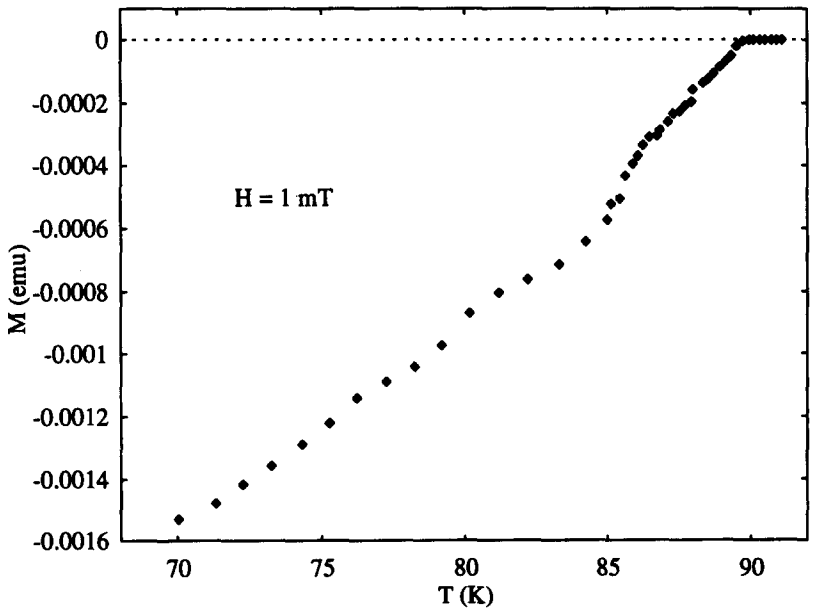

Fig. 3. ZFC magnetic susceptibility for sample T3 after reoxygenation according to the procedure b) of Fig. 1(b).

and 50 K for those textured on MgO. Samples after identical reoxygenation cycles differ substantially: those formed on Y_2O_3 (T4) display a very sharp transition at 91.5 K ($\Delta T_c = 0.5$ K) while those on MgO (T1–T3) still have a broad transition and a low $T_{c\,onset}$, see Fig. 2. Notice that this phenomena has been observed for all the samples prepared by us, three cases being presented here (T1–T3). Moreover, sample T3 has been reoxygenated twice: a first time according to the thermal cycle a) of Fig. 1(b) which provides the magnetic behaviour of Fig. 2. The second time, the sample has been reoxygenated with a step at high temperature and for longer time, see thermal cycle b) of Fig. 1(b). Fig. 3 shows the ZFC magnetisation of this sample after the second reoxygenation. Obviously, the characteristic feature of a broad transition is still present. We feel something else than reoxygenation has to be invoked to explain first the difference with Y_2O_3 substrate and second the apparent insensitivity to reoxygenation. Attempts to modify the MgO substrate have been explored. We have therefore compared fresh substrates (T1), fresh and oxygen-annealed substrates (T3) and several used substrates (T2). T1 and T3 textured samples exhibit similar behaviour (Fig. 2). For both samples, a second transition at ~ 70 K can be distinguished. The T2 textured sample shows better properties but still worse that those of the textured sample on Y_2O_3 (T4). As the same $YBa_2Cu_3O_{7-x}$ powder and thermal history were used in the four cases, substrate nature must be at the origin of this behaviour. However, a strong chemical interaction between the peritectic liquid and the substrate is observed for the Y_2O_3 case, while for MgO substrate this interaction is hardly noticeable, only the top MgO surface becoming yellowish.

The degradation of superconducting properties in these textured samples seems very similar to that previously observed in powders and also in sintered samples. For example, Maciejewski et al. [25], using oxide or metal precursors, have studied the correlation between the synthesis method of $YBa_2Cu_3O_{7-x}$ and the carbon dioxide content. In two samples having, respectively, 1582 and 286 ppm of carbon, they observed a similar $T_{c\,onset}$ but a transition width four times larger for the former sample. We consequently analysed our textured samples in terms of residual carbon content. Table 2 shows the carbon content of textured samples T1–T4 before, i.e. as grown from the MTG process, and after the typical reoxygenation cycle. Carbon content of as-grown samples was between 2700 and 1300 ppm. The sample having the highest content was the one textured on a fresh MgO substrate (T1). As a matter of fact, all samples present a higher carbon content than the starting compact used for the MTG process. Compare, for example, sample T4 (on Y_2O_3) with sample H1 used in the texturation process. This indicates that carbon was incorporated during texturation. Ceramics textured on Y_2O_3 substrate (for example T4) return to the initial carbon content (500 ppm) after reoxygenation. On the other hand, despite the fact that carbon is decreased after reoxygenation in textured samples on MgO substrates, the content is not reduced to the starting value of 600 ppm. On the contrary, it levels off at 1100 ppm for the sample on fresh MgO (T1), 800 ppm for the sample on used MgO (T2) and 1900 ppm on fresh and oxygen-annealed MgO substrate (T3). Comparing Fig. 2 and Table 2, the magnetic susceptibility behaviour correlates well with the carbon content, a higher carbon content corresponding to a broader transition width.

Table 2
Carbon content in textured ceramics

Sample name	Substrate	Carbon content as grown (ppm)	Carbon content after reoxygenation (ppm)	Transition width (K)
T1	Fresh MgO crystal	2700	1100	21
T2	Used MgO crystal	1200	800	8.5
T3	Fresh and oxygen-annealed MgO crystal	2300	1900	21
T4	Y_2O_3 polycrystalline	1300	500	0.5

4. Discussion

The results show that the anomalies on the magnetic susceptibility curves found for samples textured on MgO can be explained by the presence of residual carbon. Table 2 reveals that carbon is incorporated into the samples during the MTG process. The nature of the carbon must be different depending on the substrate because of the different behaviour with regard to the reoxygenation process. For Y_2O_3, carbon cannot be engaged into the $YBa_2Cu_3O_{7-x}$ structure since it can be easily eliminated by annealing at low temperatures in flowing oxygen. In the case of MgO, the removal of carbon is very difficult and even impossible. As an example, sample T3 has been annealed at high temperatures with a step under Ar, in conditions normally efficient at removing carbon from powders. However, Fig. 3 shows that this sample exhibits very similar behaviour after treatment, which implies that carbon has not been removed. This may be due to the lower gas-exchange ability of a solid sample with respect to a powder. However, many fast diffusion paths already exist in textured samples: growth defects, cracks, ... Therefore, the inability to remove carbon from this sample could indicate that the carbon is bonded differently than in powders. Carbon contamination in samples textured on Y_2O_3 (T4) comes from air-contained CO_2, while carbon in the T1, T2 and T3 samples is certainly supplied by the MgO substrate. Interestingly, sample T2, prepared on an already used MgO substrate, has a smaller carbon content and also the sharpest magnetisation curve among those prepared on MgO. Indeed, the texturation modifies the top layer as mentioned in Section 3. When it is not removed, it acts as a diffusion barrier layer, as is shown by the improvement in the magnetic susceptibility.

Wolf et al. [26] have shown for MgO crystals annealed at 1000°C in radioactive CO_2–CO mixtures that carbon incorporation by solid/gas exchange is very small, resulting in non-measurable solubility of carbon in bulk MgO. However, it is known that carbon is an impurity in MgO crystals, especially for those samples obtained by the sumerged arc fusion method [27]. High-purity MgO contains carbon up to 10000 ppm at the surface, even if a much lower content is found in the bulk! Thus, the source of carbon contamination in textured samples on MgO substrate is the MgO crystal and does not come from

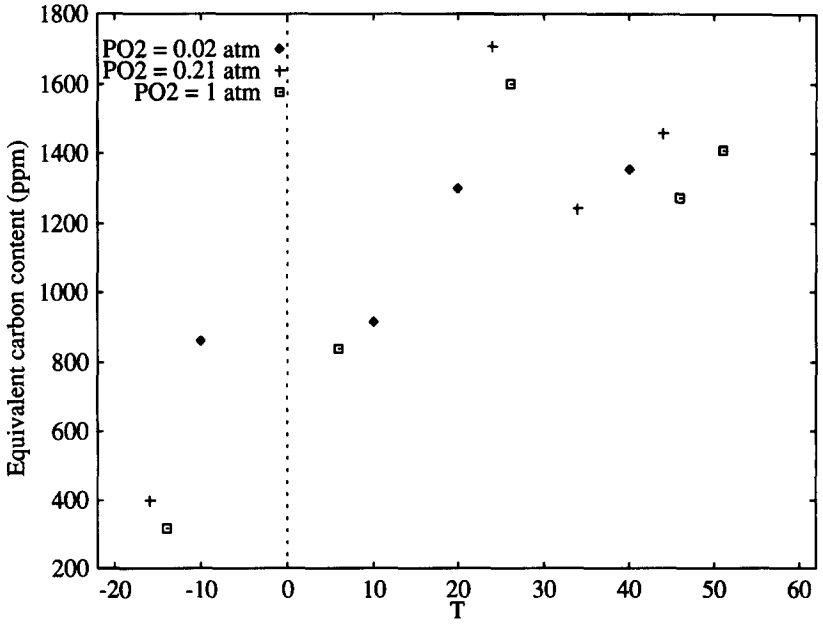

Fig. 4. Carbon content calculated from thermogravimetric measurements of Rhône-Poulenc powder annealed at different temperatures and in different atmospheres. ΔT represents the difference between the treatment temperature and the first melting temperature.

atmospheric CO_2 dissolution in MgO. Heating these crystals in air increases carbon in the upper 1–5 μm surface layer and decreases it in the bulk. By heating in oxygen, carbon can be burned out from the subsurface zone but, upon isothermal annealing at 470 K, carbon starts to diffuse from the bulk back into the subsurface zone within minutes [28]. This fact explains why more carbon is systematically found in samples using MgO substrates.

The liquid phase formed during texturation must

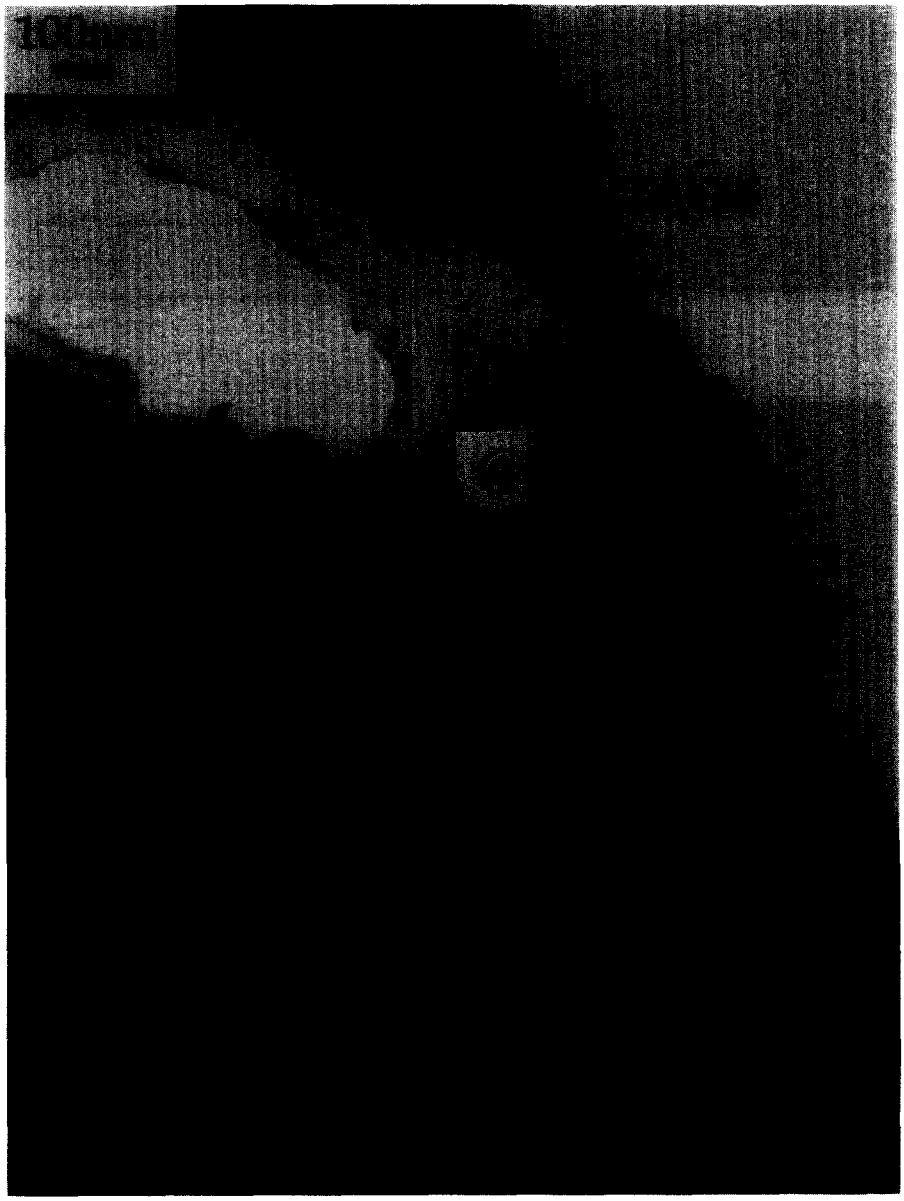

123

Fig. 5. Inter-phase region by TEM between Y_2BaCuO_5 inclusion (top) and $YBa_2Cu_3O_{7-x}$ matrix (bottom) formed after texturation on MgO. The inter-phase structure is perturbed and contains an anomalously large amount of carbon.

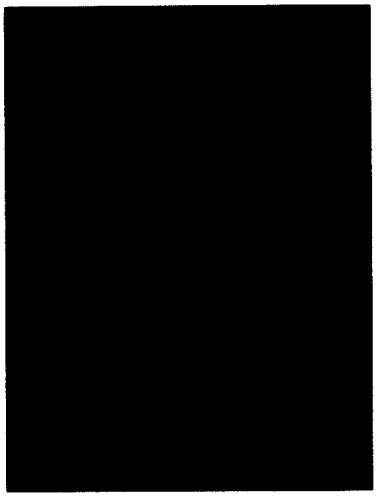

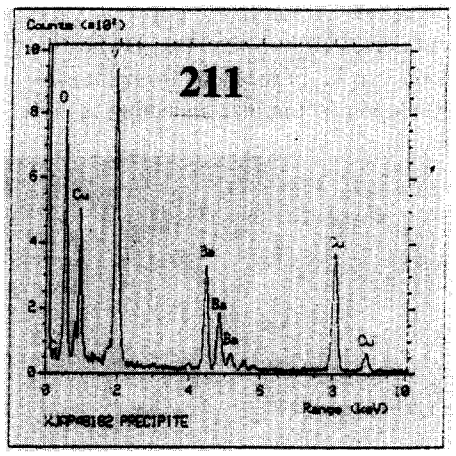

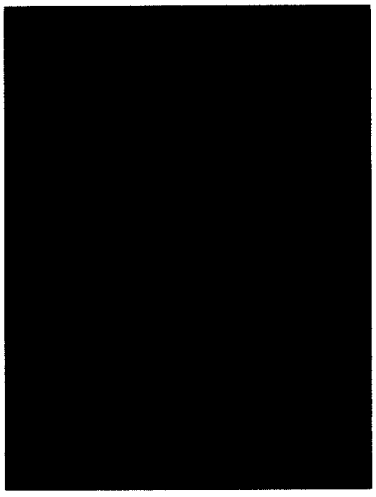

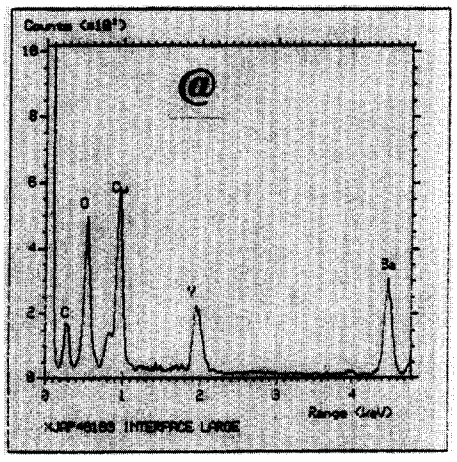

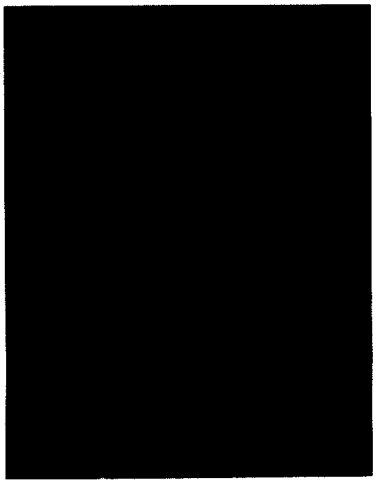

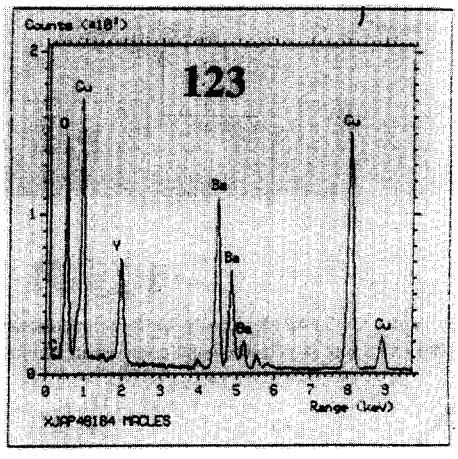

Fig. 5 (continued).

play an active role on the carbon retention from the MgO substrates. The affinity of the liquid phase toward carbon is indicated by the high carbon content determined for the RP2 ceramic which has been sintered at 950°C in oxygen. The first melting event for the Rhône-Poulenc ceramics appears at approximately 925°C in oxygen atmosphere. This suggests that carbon cannot be eliminated if a liquid phase is generated during the firing treatment. This phenomenon is shown in Fig. 4 (drawn from Ref. [29]) where is displayed the carbon content calculated from thermogravimetric measurements of the same Rhône-Poulenc powder fired at different temperatures and in different atmospheres. ΔT represents the difference between the treatment temperature and the first melting temperature. It is clearly shown that in all cases a better decarbonatation is possible up to liquid phase apparition.

For samples prepared on MgO (T1–T3), carbon must be engaged within the $YBa_2Cu_3O_{7-x}$ structure during crystallisation because it affects an intragranular property, the magnetic susceptibility. Nanoprobe chemical analysis has confirmed that carbon is in the $YBa_2Cu_3O_{7-x}$ structure and not present as an intergranular phase [22]. This carbon is not eliminated by annealing in non-oxidising atmosphere, contrarily to the metastable oxycarbonate powder. In this phase, the CO_3^{2-} group is located in the centre of the basal CuO square (also called Cu(1)) [15]. However, in the textured samples, carbon might have a similar configuration to the oxycarbonate family with nominal composition $Y_nBa_{2n}Cu_{3n-1}CO_3O_{7n-3}$ [18]. In this phase, a CO_3^{2-} group replaces the CuO_4 square-planar group, or rather copper atoms are simply replaced by carbon atoms linked to oxygen atoms of the $YBa_2Cu_3O_{7-x}$ structure. In this case, carbon is incorporated into the structure in a substitution site and not in an interstitial one as in the so-called gel powder discussed above. This explains why carbon cannot be easily removed because it would be then necessary to destroy the $YBa_2Cu_3O_{7-x}$ structure. In addition, by quantitative analysis with an electron microprobe we found a systematic copper deficit in samples obtained from a liquid phase, and this can facilitate carbon entrapment [30]. A carbon content between 1900 and 800 ppm agrees with a nominal composition with n between 10 and 20. This carbon which cannot be homogeneously distributed explains the broad transition temperature. Carbon species present in insertion or in substitution in the $z = 0$ plane affect T_c through a modification of the hole doping of the CuO_2 planes. Moreover, the introduction of the carbonate group impedes the long-range development of Cu–O chains along the b-direction. In any case, the CO_3^{2-} group blocks up the O(1) site, which clarifies why all these oxycarbonate phases are apparently inert to the reoxygenation process.

It must be noticed that only millimetric textured grains were achieved on MgO while textured grains of larger dimensions were possibly reached on Y_2O_3. Carbon contamination of the liquid may be one of the reasons. This effect is more obvious in the bottom part of the sample where only small single domains are found embedded in copper-rich regions (composed with the peritectic liquid). In contrast, in the top part, far from the MgO substrate, 123 grains of larger dimensions are noticed. The microstructures of such grains have been studied by TEM [22]. As a matter of fact, the $YBa_2Cu_3O_{7-x}$ structure is perturbed when an anomalously large amount of carbon is present. One such example is shown in Fig. 5, a bright field image of an area containing $YBa_2Cu_3O_{7-x}$ and a grain of Y_2BaCuO_5 inclusion. Curiously, the area marked @ which is far from the interface, 200 nm, has a different aspect than the area just below where the usual contrast due to twins is visible. These regions have been analysed by electron diffraction and EDS punctual analysis (nanosize probe). Two conclusions come out:

(1) the $YBa_2Cu_3O_{7-x}$ perturbed zone contains carbon while the Y_2BaCuO_5 inclusion and the non-perturbed $YBa_2Cu_3O_{7-x}$ region do not;

(2) the perturbed zone has a modified structure which is tetragonal.

Such perturbed areas presumably impede long-range texturation. Consequently, the recommendation for using MgO crystals in melt processes due to their unreactivity [31,32] must be questioned if the MgO quality is not verified.

5. Conclusions

The anomalies on magnetic susceptibility curves found in $YBa_2Cu_3O_{7-x}$ samples textured on MgO substrates have their origin in the presence of resid-

ual carbon. A carbon content smaller than about 600 ppm was necessary to obtain a sharp superconducting transition at 91.5 K. A qualitative correlation between the transition width and the carbon content was shown. Liquid phase plays an active role in carbon incorporation in the $YBa_2Cu_3O_{7-x}$ structure from the MgO substrate during texturation. Carbon in powders and sintered ceramics can be eliminated if precursor processing is realised carefully. Particularly, liquid phase formation must be avoided during the firing treatment.

In general, we suggest that if liquid phase is prevented during processing, carbon is incorporated in an interstitial site creating an oxycarbonate metastable phase which is transformed into $YBa_2Cu_3O_{7-x}$ phase by annealing at high temperatures. However, if liquid phase is formed, carbon is incorporated inside the $YBa_2Cu_3O_{7-x}$ structure into a substitution site (carbon substitutes copper atoms) during crystallisation. Carbon removal from this more stable oxycarbonate form cannot be possible without crystal structure destruction.

Acknowledgements

This work was financially supported by the French co-operative research program: "CPR-Courants Forts dans les Supraconducteurs à Haut T_c". One of the authors (FJG) is very grateful to the European Union for a Postdoctoral Fellowship (Human Capital and Mobility).

References

[1] I. Sargankova, P. Diko, M. Timko, M. Cernik and J. Mihalik, Solid State Ionics 63–65 (1993) 852.
[2] J.E. Blendell, C.K. Chiang, D.C. Cranmer, S.W. Freiman, E.R. Fuller Jr., E. Drescher-Krasicka, W.L. Johnson, H.M. Ledbetter, L.H. Bennett, L.J. Swartzendruber, R.B. Marinenko, R.L. Myklebust, D.S. Bright and D.E. Newbury, Adv. Ceram. Mater. 2 (1987) 512.
[3] T.M. Shaw, D. Dimos, P.E. Batson, A.G. Schrott, D.R. Clarke and P.R. Duncombe, J. Mater. Res. 5 (1990) 1176.
[4] Y. Masuda, R. Ogawa, Y. Kawate, K. Matsubara, T. Tateishi and S. Sakka, J. Mater. Res. 8 (1993) 693.
[5] J. Karpinski, K. Conder, H. Schwer, Ch. Krüger, E. Kaldis, M. Maciejewski, C. Rossel, M. Mali and D. Brinkmann, Physica C 227 (1994) 68.
[6] L. Zhang, J. Chen, H.M. Chan and M.P. Harmer, J. Am. Ceram. Soc. 72 (1989) 1997.
[7] J.M. Heintz, C. Magro, K. Frohlich, P. Dordor and J.P. Bonnet, Eur. J. Solid State Inorg. Chem. 27 (1990) 703.
[8] N. Rüffer, G. Kaiser and H.R. Khan, Cryogenics 33 (1993) 124.
[9] Y. Gao, K.L. Merkle, C. Zhang, U. Balachandran and R.B. Poeppel, J. Mater. Res. 5 (1990) 1363.
[10] K. Borowiec, J. Przyluski and K. Kolbrecka, J. Am. Ceram. Soc. 74 (1991) 2007.
[11] K. Brzezinska, S. Bruckenstein, L.J. Klemptner and J.D. Hodge, J. Mater. Sci. 28 (1993) 5155.
[12] T.B. Lindemer, C.R. Hubbard and J. Brynestad, Physica C 167 (1990) 312.
[13] P. Karen and A. Kjekshus, J. Solid State Chem. 94 (1991) 298.
[14] M.A. Rodriguez, J.J. Simmins and R.L. Snyder, J. Mater. Res. 8 (1993) 415.
[15] F.J. Gotor, P. Odier, M. Gervais, J. Choisnet and Ph. Monod, Physica C 218 (1993) 429.
[16] X.Z. Wang, M. Henry, J. Livage and I. Rosenman, Solid State Commun. 64 (1987) 881.
[17] P. Barboux, I. Campion, S. Daghish, J. Livage, J.L. Genicon, A. Sulpice and R. Tournier, J. Non-Cryst. Solids 147–148 (1992) 704.
[18] Ph. Boullay, B. Domenges, M. Hervieu and B Raveau, Chem. Mater. 5 (1993) 1683.
[19] M. Hervieu, Ph. Boullay, B. Domenges, A. Maignan and B. Raveau, J. Solid State Chem. 105 (1993) 300.
[20] B. Domenges, M. Hervieu and B. Raveau, Physica C 207 (1993) 65.
[21] F. Izumi, K. Kinoshita, Y. Matsui, K. Yanagisawa, T. Ishigaki, T. Kamiyama, T. Yamada and H. Asano, Physica C 196 (1992) 227.
[22] N. Pellerin, F.J. Gotor, P. Odier, J. Ayache, A. Fert, E. Cazy and J.P. Bonnet, Physica C 235–240 (1994) 381.
[23] A. Douy and P. Odier, Mater. Res. Bull. 24 (1989) 1119.
[24] F.J. Gotor, Y. Ayache, N. Pellerin and P. Odier, unpublished data.
[25] M. Maciejewski, A. Baiker, K. Conder, Ch. Krüger, J. Karpinski and E. Kaldis, Physica C 227 (1994) 343.
[26] I. Wolf and H.J. Grabke, Solid State Commun. 54 (1985) 5.
[27] F. Freund, G. Debras and G. Demortier, J. Am. Ceram. Soc. 61 (1978) 429.
[28] G. Demortier, Nucl. Instr. and Meth. in Phys. Res. B 66 (1992) 51.
[29] E. Cazy, D. Bahloul and D. Smith, J. Phys. III (Paris) 4 (1994) 2105.
[30] F.J. Gotor, N. Pellerin and P. Odier, unpublished data.
[31] C.J. Kim, K.B. Kim and G.W. Hong, Supercond. Sci. Technol. 7 (1994) 812.
[32] Ch. Krauns, M. Tagami, Y. Yamada, M. Nakamura and Y. Shiohara, J. Mater. Res. 9 (1994) 1513.